Topological High-Entropy Disorder Mechanical Metamaterial Made of Honeycomb with Hat Cell

Xiao Lin Guo and Bo Hua Sun *

Posted Date: 8 April 2025

doi: 10.20944/preprints202407.1532.v2

Keywords: monotile; einstein; metamaterials; entropy; disorder; strength of materials

 doi:10.20944/preprints202407.1532.v2

Article

Topological High-Entropy Disorder Mechanical Metamaterial Made of Honeycomb with Hat Cell

Xiao Lin Guo [1,2] and Bo Hua Sun [2,3,*]

[1] School of Civil Engineering, Institute of Mechanics and Technology, Xi'an University of Architecture and Technology, Xian 710055, China
[2] Beijing Institute of Nanoenergy and Nanosystems, Chinese Academy of Sciences, Beijing 101400, China
[3] School of Sciences, Institute of Mechanics and Technology, Xi'an University of Architecture and Technology, Xian 710055, China
* Correspondence: sunbohua@binn.cas.cn

Abstract: People have always hoped to be able to fill an entire plane with 'single unit cells' without periodicity. This wish was realized after the mathematician discovered a 13-sided "single cell" named 'einstein', we also refer to it as a hat tiling. These non-periodic tessellations generally exhibit anisotropic properties, making them superior in terms of mechanical performance compared to periodic structures, the application of non-periodic hat tiling in the study of honeycomb metamaterial structures. From the perspective of information entropy, the reason behind the improved mechanical properties of these structures is the higher entropy associated with non-periodic configurations. To quantify the disorder of non-periodic structures, we propose an entropy expression for the 'einstein' metamaterial. To demonstrate the mechanical properties of these high-entropy structures, we fabricate specimens using 3D printing and conducte mechanical experiments. For comparative analysis, we also use ABAQUS to perform finite element analysis of the problem. The research results reveal that the mechanical properties of high-entropy structures created by the non-periodic stacking of cells are significantly improved compared to those of low-entropy structures created by periodic stacking. The conclusions drawn from the study of individual issues are generalizable and may be of assistance in future material and structural design.

Keywords: monotile; einstein; metamaterials; entropy; disorder; strength of materials

1. Introduction

A roadside wall on the way to the Colosseum in Rome is made from blocks of different shapes as shown in Figure 1, possessed anisotropic properties within its surface, which obviously endowed it with excellent shear resistance. People have always hoped to be able to fill an entire plane with "single unit cells" without periodicity. However, it is difficult to cover the entire wall using only one type of block. This was realized after the mathematician discovered a 13-sided "single unit cell" named hat as shown in Figure 2. Although the name 'einstein' conjures up the iconic physicist, it comes from the German ein Stein, meaning 'one stone', referring to the single tile. The 'einstein' sits in a weird purgatory between order and disorder. Though the tiles fit neatly together and can cover an infinite plane, they are aperiodic, meaning they can't form a pattern that repeats [1–3].

 doi:10.20944/preprints202407.1532.v2

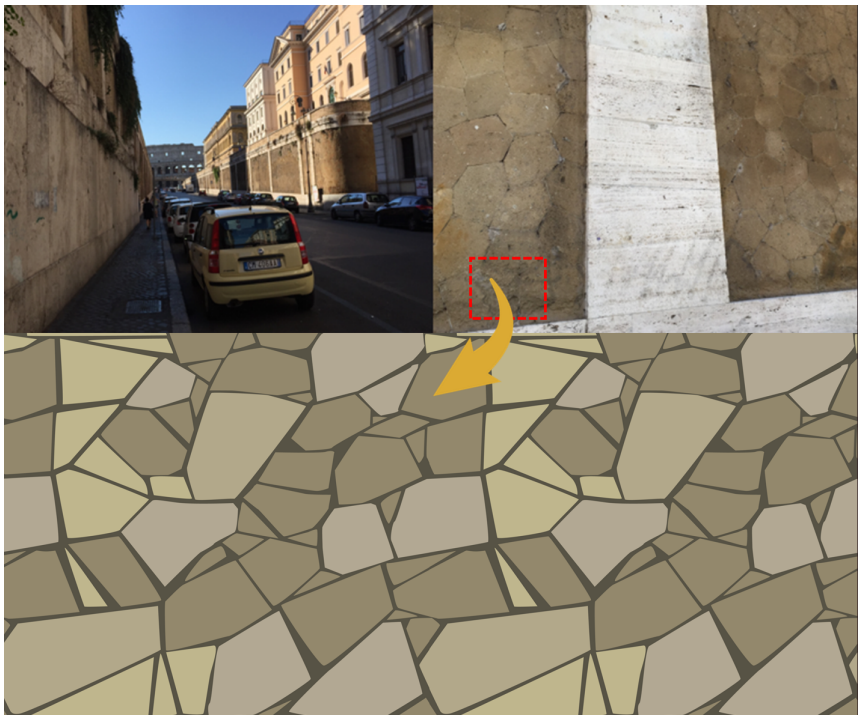

Figure 1. A roadside wall on the way to the Colosseum in Rome, photos took by Bo Hua Sun.

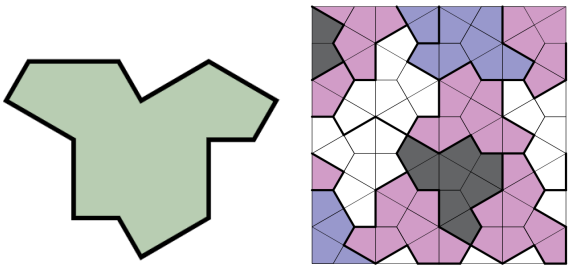

Figure 2. Left: Monotile: A 13-sided tile called hat. Right: The hat forms a pattern that covers an infinite plane yet it cannot repeat [1,2].

Nonrepeating patterns can have real-world connections. Materials scientist Dan Shechtman won the 2011 Nobel Prize in chemistry for his discovery of quasicrystals [4], materials with atoms arranged in an orderly structure that never repeats, often described as analogs to Penrose's tilings [5].

Metamaterials are materials or devices with artificial structures that can control and utilize physical mechanisms in novel ways, achieving properties or functions that are not possible with natural materials. Metamaterials (or a type of mechanism with functionality) possess unprecedented characteristics, which have promoted the development of advanced devices and equipment. Mechano-metamaterials, with unique mechanical properties, can provide some novel functional characteristics, such as high energy absorption efficiency, ultra-toughness, complex bistable states, tunable stiffness, negative thermal expansion, and tension-compression behavior, etc. For examples, Bertoldi et al. [6] discuses the main fundamental mechanisms underlying mechanical metamaterials. Ashby [7] studies the bending-dominated and stretching-dominated density scaling of mechanical properties in cellular solids. Lakes [8] provides an introduction to auxetic materials (foam structures) showing negative Poisson's ratio. Hanifpour et al. [9] provides a systematic study of the role of disorder in auxetic metamaterials.

The standard design strategy for mechanical metamaterials, based on the periodic replication of unit cells, appears in contrast to many functionally efficient but structurally disordered biological materials observed in nature and mega engineering structures as shown in Figure 3, this is incorporating disorder into their design can provide improved functionalities over ordered structures. This

 doi:10.20944/preprints202407.1532.v2

suggests that including randomness in meta material design could provide advantages that are yet to be explored [10].

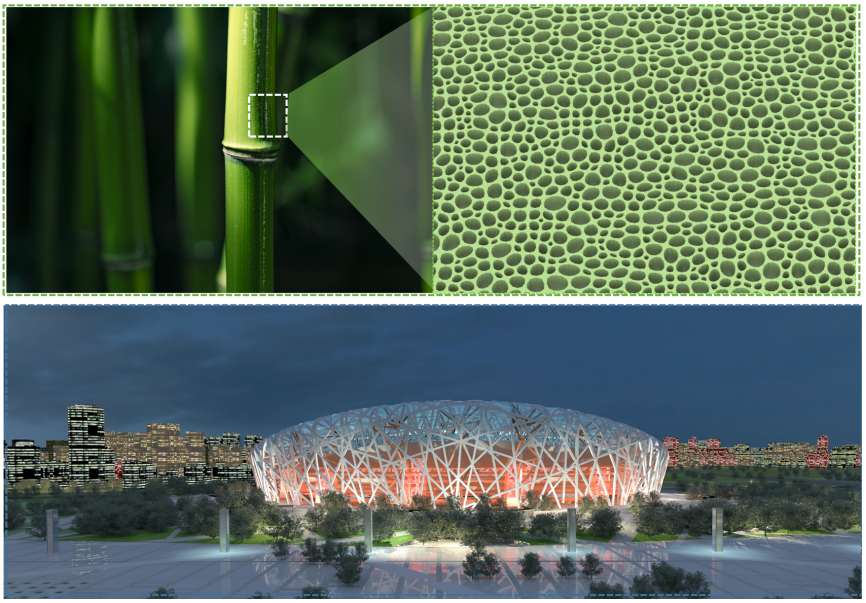

Figure 3. Top left: Bamboo cellulose. Top right: Natural wood cellulose. Bottom: The Bird's Nest in Beijing.

Due to the benefits of disorder, non-periodicity, or randomness in improving material performance, there has been increasing interest. Tüzes et al. [11] study the fracture problem and state that disorder is beneficial for influencing local disorder on strain localization and ductility in strain softening materials. Bonfanti et al. [12] demonstrate how to generate disordered metamaterials using Monte Carlo simulations combined with deep learning. Liu et al. [13] show how to design irregular architected metamaterials with a random growth algorithm. Li and Sun [14,15] study the optimization of a lattice structure inspired by glass sponge, and low-speed impact response of sandwich panels with bio-inspired diagonal-enhanced square honeycomb core. Wu and Sun [16] study on functional mechanical performance of array structures inspired by cuttlebone. Guo and Sun [17,18] study assembly and disassembly mechanics of elastic snap-fit cells, the detachable connection mechanics of thin-walled cylindrical/segmented torus snap fit docking. Wei and Sun [19,20] study pull-out mechanical properties of the Jigsaw connection of diabolical ironclad Beetle's Elytra and cylindrical mechanical metamaterials with biomimetic honeycomb units of the diabolical ironclad beetle. Clarke et al. [21] investigate an isotropic zero Poisson's ratio metamaterial based on the aperiodic hat monotile. Moat [22] study a class of aperiodic honeycombs with tuneable mechanical properties. Wang et al. [23] study the unprecedented strength enhancement observed in interpenetrating phase composites of aperiodic lattice metamaterials. Naji and Abu Al-Rub [24] study the effective elastic properties of novel aperiodic monotile-based lattice metamaterials. Jung et al. [25] study aperiodicity is all you need: aperiodic monotiles for high-performance composites.

2. Entropy of Topological Disorder Mtamaterials/Strucures

From a thermodynamic perspective, disorder can be quantified by borrowing the concept of thermodynamic entropy. Clearly, for periodic structures, the entropy is relatively low, whereas for disordered structures, the entropy should be relatively high. Therefore, to obtain supramaterials with superior mechanical properties, one design philosophy is to incorporate high entropy, therefore Sun [26,27] proposed a conceit of high-entropy structural mechanics by in two seminars. However, complete disorder would present challenges for manufacturing and controlling mechanical properties. An ideal situation is that any structure can be constructed by stacking montile; hat is currently the best choice for these montile [1,2]. The question arises as to how to define the entropy of structures composed of hat units. The difficulty here is how to characterize the change in entropy that occurs

 doi:10.20944/preprints202407.1532.v2

when the topology is altered while maintaining the material's properties unchanged. This is different from the definition of entropy in high-entropy materials, which is calculated based on the ratio of components from different materials.

2.1. Entropy Definition of Topological Disorder Metamaterials/Strucures

Entropy definition of topological disorder metamaterials/strucures: Defining entropy for disordered metamaterials/strucures is complicated because it requires understanding the disorder and randomness within the system. For topological disordered cells, the entropy might also involve the topology and geometry of the disorder. This could mean considering the spatial distribution of the cells, their relative orientations, and any patterns or correlations that may emerge.

The structure composed of cells named hat exhibits a uniformity in size, shape, and topology among its cells. The only difference lies in each cell's unique orientation. This diversity in directionality signifies disorder and forms the basis for our definition of entropy.

By coloring the hat cells with the same orientation within the structural diagram with the same color, each color represents a specific orientation. Therefore, the entropy of this structure can be defined as the sum of the product of each color's proportion.

The disorder metamaterial entropy can be characterised by Shannon entropy [28], which quantifies the amount of uncertainty associated with a random variable. Claud Shannon's paper 'A mathematical theory of communication' [28] published in July and October of 1948 is the Magna Carta of the information age. Shannon's discovery of the fundamental laws of data compression and transmission marks the birth of information theory.

The Shannon entropy H of a discrete random variable X and probability mass function $P(X)$ is defined as: $H(X) = -P(X)\log_b P(X)$, where $P(X)$ is the probability of the random variable. The logarithm base b is usually 2, but it can be any base. The Shannon entropy entropy $H(X)$ is always non-negative and additivity, namely, if two random variables X and Y are independent, then the entropy of their combination is the sum of their individual entropies: $H(X,Y) = H(X) + H(Y)$.

Assuming there are a total of N hat cells, with N_a cells facing upwards and N_b cells facing downwards, that is, $N = N_a + N_b$. If the proportion of each orientation among the cells facing upwards is $p_i (i = 1, 2, ..., n)$, then the entropy of each cell is defined as $P_i = p_i/N_a$, the total entropy of the facing upwards can be added up as follows:

$$H_a = -\sum_{i=1}^{K_a} \frac{p_i}{N_a} \log_2 \frac{p_i}{N_a}, \tag{1}$$

where K_a is the number of same-orientation in type-a. (Here it is assumed that $0 \log_2 0 = 0$).

If the proportion of each orientation among the cells facing downwards is $q_i (i = 1, 2, ..., m)$, then the entropy of each cell is defined as $P_i = q_i/N_b$, the total entropy of the facing downwards can be added up as follows:

$$H_b = -\sum_{i=1}^{K_b} \frac{q_i}{N_b} \log_2 \frac{q_i}{N_b}, \tag{2}$$

where K_b is the number of same-orientation in type-a.

By considering the weightage of the upwards-facing cells as $\frac{N_a}{N_a+N_b}$ and the downwards-facing cells as $\frac{N_b}{N_a+N_b}$, the total entropy can be obtained as:

$$H = \frac{N_a}{N_a + N_b} H_a + \frac{N_b}{N_a + N_b} H_b. \tag{3}$$

The above expression for calculating entropy is for the case of discrete configurations. If it is a continuum, the above expression can simply be modified into an integral form. For example, the entropy of a planar continuum is: $H = -\int_S P(x,y) \log_2 P(x,y) dxdy$.

 doi:10.20944/preprints202407.1532.v2

2.2. Entropy of the Hat Honeycomb Metamaterial

We consider the two-dimensional plane of the hat honeycomb metamaterial designed as described above, as illustrated in Figure 4. Since the hat tiling is obtained by rotation and mirroring of a non-periodic arrangement, we divide the hat tiling into two types, labeled as type-a and type-b (where type-a and type-b are mirror images of each other). The line connecting the two outermost points of the hat tiling cell is AB/BA, and the rotation angle of the hat tiling with respect to the x-axis (clockwise rotation is positive, counterclockwise rotation is negative) is defined as the relative rotation angle θ of the hat tiling. Only the rotation of the complete hat tiling cell is considered within the entire plane system. Table 1 lists the relative rotation angles and quantities of the two types of hat tilings. In the same scenario, the relative rotation angle of each square cell in the two-dimensional plane of the square honeycomb metamaterial is 0.

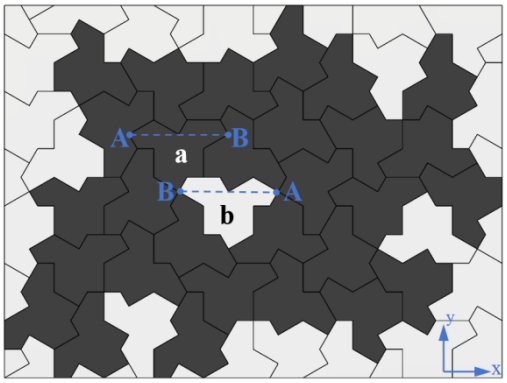

Figure 4. The hat honeycomb metamaterial two-dimensional plane definition.

Table 1. Orientation and number of hat tiling.

Angle	0°	60°	−60°	120°	−120°	180°		
	p_1	p_2	p_3	p_4	p_5	p_6	N	K
type-a	5	8	6	5	2	3	29	6
type-b	1	1	0	2	0	1	5	4

Applying the entropy definition in Eq.1 to the Type-a (black color in Figure 4), we have its entropy as follows

$$\begin{aligned} H_a = &-(\frac{5}{29}\log_2\frac{5}{29} + \frac{8}{29}\log_2\frac{8}{29} + \frac{6}{29}\log_2\frac{6}{29} \\ &+ \frac{5}{29}\log_2\frac{5}{29} + \frac{2}{29}\log_2\frac{2}{29} + \frac{3}{29}\log_2\frac{3}{29}) \\ &\approx 2.461982945. \end{aligned} \tag{4}$$

Applying the entropy definition in Eq.2 to the Type-a (white color in Figure 4), we have its entropy as follows

$$\begin{aligned} H_b = &-(\frac{1}{5}\log_2\frac{1}{5} + \frac{1}{5}\log_2\frac{1}{5} + \frac{2}{5}\log_2\frac{2}{5} + \frac{1}{5}\log_2\frac{1}{5}) \\ &\approx 1.921928095. \end{aligned} \tag{5}$$

By considering the weightage of the upwards-facing cells as $\frac{N_a}{N_a+N_b}$ and the downwards-facing cells as $\frac{N_b}{N_a+N_b}$, the total entropy can be obtained as:

$$H_{einstein} = \frac{29}{34}H_a + \frac{5}{34}H_b = 2.38. \tag{6}$$

 doi:10.20944/preprints202407.1532.v2

For any periodic structure as shown in Figure 5, since the cells do not rotate, all cells have the same directionality, that is, $p_i = N_a\ (i = 1, 2, 3, ...N_a)$, which implies $\frac{p_i}{N_a} = 1$. Therefore, the entropy of the periodic structure is zero, that is,

$$H_{periodic} = -\sum_{i=1}^{K_a} \frac{p_i}{N_a} \log_2 \frac{p_i}{N_a} = -\sum_{i=1}^{K_a} (1) \log_2 (1) = 0. \tag{7}$$

The quantitative study from here reveals that the entropy of non-periodic structures is much higher than that of periodic structures. Since high entropy corresponds to anisotropy in materials, generally, anisotropic materials have better mechanical properties than isotropic materials. Therefore, structures with high entropy have superior mechanical properties compared to those with low entropy. This allows for the prediction of a material's mechanical properties in advance, without the need for specific experiments and numerical simulations, by calculating the structural information entropy.

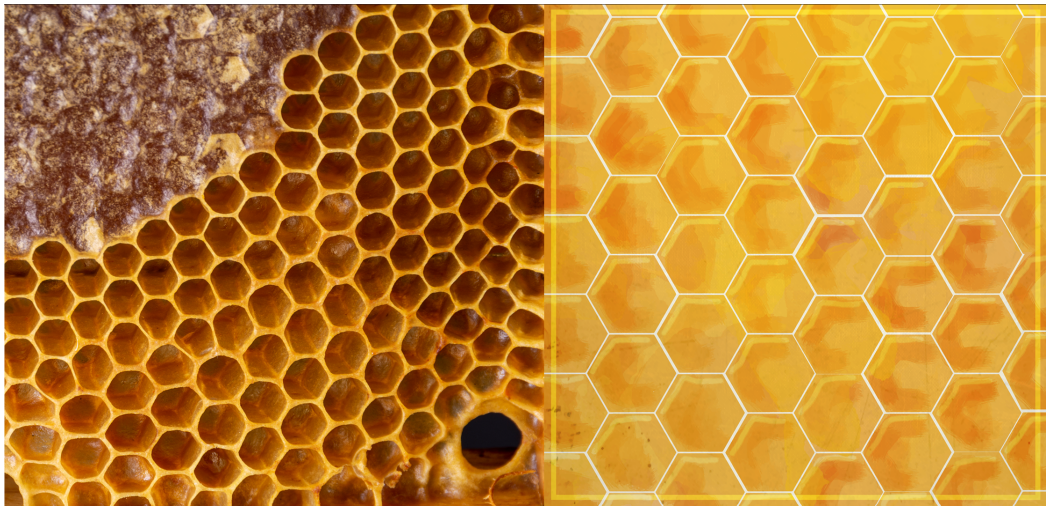

Figure 5. A periodic structure: Honeycomb. The periodic structure is generated by a unit cell through translation without rotation, hence it is generally isotropic.

3. Sample Manufacturing and Mechanical Testing

3.1. Structural Design

The hat tiling is applied as a honeycomb unit in the design of metamaterials, named the hat honeycomb. As shown in Figure 6, the two-dimensional microstructure of the hat honeycomb is a 13-sided polygon, consisting of 16 right-angled triangle units. The sides of the 13-sided unit are constructed from the sides of the right-angled triangles, with the parameters defined as follows [3]:$\tan\theta = \frac{l_2}{l_1} = \frac{1}{\sqrt{3}}$. The established hat honeycomb is formed by rotating the 13-sided units along the x,y directions and mirroring the non-periodic arrangement.

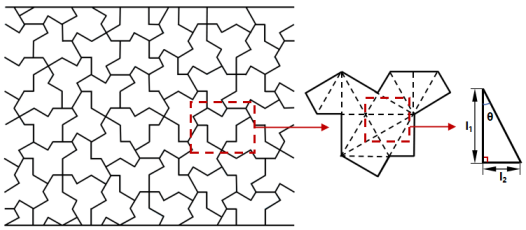

Figure 6. The hat honeycomb and one of its cells.

To better understand the mechanical properties and energy absorption of the hat honeycomb (Figure 7(a)), a honeycomb structure with regular square cells was also established for comparison. The square honeycomb metamaterial is composed of square cells arranged periodically along the x,y directions, as shown in Figure 7(b).

 doi:10.20944/preprints202407.1532.v2

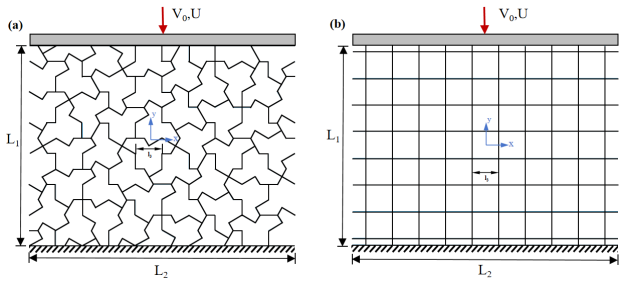

Figure 7. The geometric configurations and boundary conditions of two types of honeycomb metamaterials.

A series of geometric parameters were established, where the side lengths of the right-angle triangle cells are $l_1 = 3\sqrt{3}mm$, $l_2 = 3mm$, and the side length of the square cells is $l_3 = 9mm$. The other parameters of the two honeycomb structures are the same, including the cell wall thickness $t = 0.6mm$ and the out-of-plane thickness $h = 16mm$.

3.2. Sample Manufacturing

The experimental specimens were fabricated using the Chinese-Swedish iSLA880 photocurable laser 3D printer, with white photoresin as the printing material, to print two configurations of honeycomb metamaterials. To ensure accurate and efficient printing, the process was carried out at room temperature with a printing layer thickness $0.1mm$. Figure 8 shows the specimens of the two honeycomb metamaterials, both with dimensions of $90mm \times 30\sqrt{3}mm \times 16mm$.

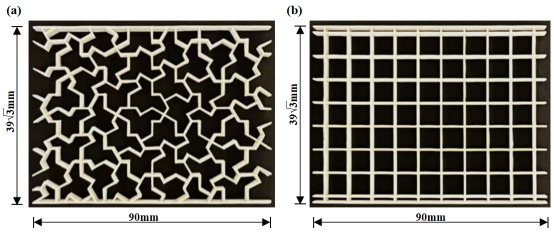

Figure 8. Two types of 3D-printed honeycomb metamaterial specimens:(a)The hat honeycomb,(b)The square honeycomb,both thicknesses are $t = 0.6mm$.

3.3. Mechanical Testing

First, the material properties of the honeycomb structure were tested, and then these obtained material properties were applied to finite element simulations to model the compression deformation process of the two types of honeycomb structures. Specimens were prepared using a Sweden-China iSLA880 photocurable laser 3D printer in the shape of a dumbbell, with white photocurable resin as the printing material. Quasi-static isothermal tensile experiments were conducted at room temperature using a universal testing machine (MTS) to determine the stress-strain curve, thereby obtaining the tensile performance parameters of the material. The experimental equipment for determining the tensile specimens are shown in Figure 9 and the stress-strain curve are shown in Figure 10.

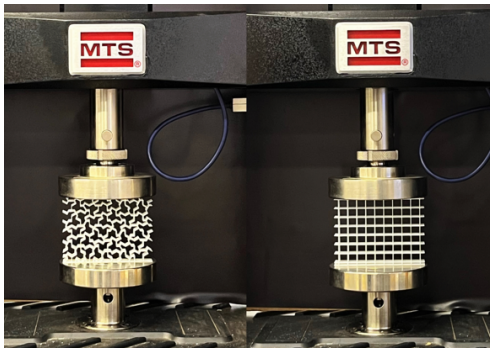

Figure 9. Experimental set up.

 doi:10.20944/preprints202407.1532.v2

The unit design of the metamaterial structure determines the mechanical properties and energy absorption capacity of the metamaterial. To evaluate the mechanical properties and energy absorption capabilities of the two honeycomb metamaterials, we conducted quasistatic compression tests at room temperature using an MTS universal testing machine. The loading rate was set at $4mm/min$, and the loading process continued until the specimens reached their compaction stage. To ensure the accuracy of the experiments, the same type of specimen was tested under the same conditions three times. The deformation process of the specimens during compression was recorded using a camera.

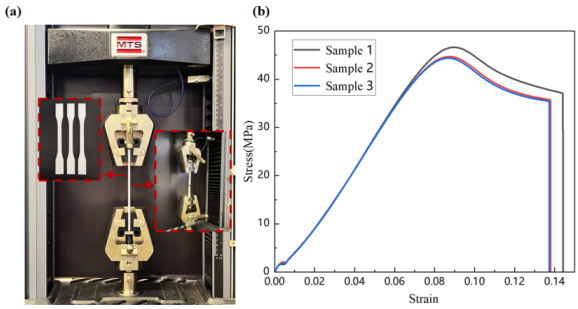

Figure 10. (a) Tensile specimen and testing equipment, (b) Stress-strain curve of the tensile specimen.

4. Numerical Simulation Compared with Experiment

Numerical simulation compared with experiment: The compression and deformation mechanism of two types of honeycomb metamaterials were studied by ABAQUS/EXPLICIT 2023 simulation software. Based on the designed geometries, three-dimensional finite element models of the honeycomb metamaterials with different cells were established. The finite element models were meshed using shell elements (S4R). To simulate the compression experimental conditions in the numerical simulation, rigid plates were placed on the top and bottom surfaces of the structure. As shown in Figure 11, the longitudinal direction within the finite element structure's plane is the y direction, and the transverse direction within the plane is the x direction. The rigid plate on the top surface was moved downward along the y direction at a constant velocity of $V_0 = 4mm/min$(the overall displacement of the structure is U), while the rigid plate on the bottom surface was fully fixed. In the finite element simulation, a friction coefficient $\mu = 0.3$ was used, with a general contact implementation, normal contact set as hard contact, and penetration was not allowed.

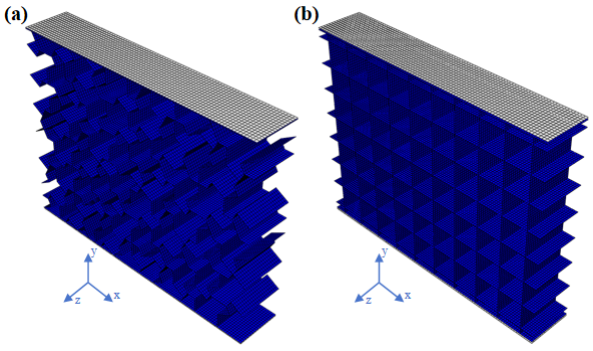

Figure 11. The finite element model.

4.1. Compression Deformation Characteristics and Mechanical Properties

The experimental and simulated deformation processes of the hat honeycomb and square honeycomb metamaterials are shown in Figure 12. We were able to clearly observe the deformation patterns of the two honeycomb metamaterials during compression and evaluate their mechanical properties.

Figure 12(a) shows the experimental and simulated deformation processes and comparisons of the hat honeycomb metamaterial. It can be clearly observed that due to the non-periodic arrangement of the hat cells, there is a trend of mutual interference and resistance to deformation during the

 doi:10.20944/preprints202407.1532.v2

compression process, and the honeycomb metamaterial generally has a stable deformation pattern. The entire structure undergoes axial compression-contraction, and the hat honeycomb metamaterial exhibits excellent mechanical properties. As the amount of compression increases, the structure begins to collapse, and ultimately the structure is densely solidified, the overall deformation of the structure is uniform. The deformation of this finite element model is consistent with the experimental results. Figure 12(b) presents the experimental and simulated deformation processes and comparisons of the square honeycomb metamaterial. It can be clearly observed that due to the asymmetric deformation of the square honeycomb metamaterial, the nodes at the structure's edges fail prematurely, leading to a tendency of the overall structure to tilt primarily to one side and overall buckling deformation. The deformation of this finite element model is also consistent with the experimental results. As shown in Figure 13,The hat cell can resist lateral deformation through coordinated bending deformation at the concave corners, while the square cell exhibits lateral expansion deformation due to the bending deformation of its walls.In summary, compared to the traditional periodically arranged square honeycomb metamaterials, the non-periodically arranged hat honeycomb metamaterials have a more stable compression deformation process,.

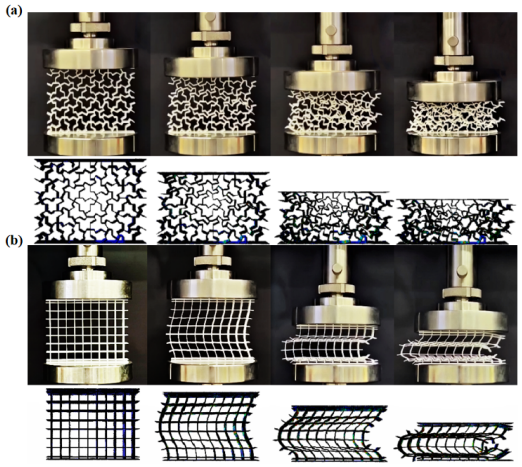

Figure 12. Comparison of experimental and simulated deformation of two honeycomb metamaterials under room temperature compression.

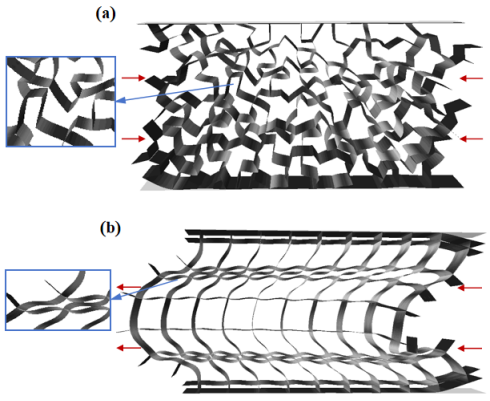

Figure 13. Macroscopic and microscopic deformation patterns of two honeycomb metamaterials.

To evaluate the compressive mechanical properties of the hat honeycomb and square honeycomb metamaterials at room temperature, we have plotted the force-displacement curves of the two honeycomb metamaterials at room temperature, including both experimental and simulated results, as shown in Figure 14.

Finite element simulations successfully predicted the force-displacement relationships during in-plane compression of the two honeycomb metamaterials. Figure 14 confirms the good agreement

 doi:10.20944/preprints202407.1532.v2

between the simulated curves and the experimental force-displacement curves of compression. We only compare the force-displacement curves for the overall vertical displacement $U < 38mm$, as after $U > 38mm$ the force increases sharply due to the compaction of the honeycomb structure. It can be observed from Figure 13 that the force-displacement curve of the hat honeycomb metamaterial rises relatively slowly in the initial stage, indicating its lower load-bearing capacity at small displacements. As the displacement increases, the amplitude of the force increase gradually becomes larger, rising basically steadily without any significant peaks and valleys (the sharp points in the red curve of the figure are due to local fractures, which are related to the material properties selected in the experiment), and the overall structure has very good stability. In contrast, the load-bearing capacity of the square honeycomb structure increases rapidly at smaller displacements, followed by buckling instability of the structure. After that, as the displacement increases, the stiffness and strength of the hat honeycomb metamaterial are significantly higher than those of the square honeycomb metamaterial. In summary, compared to the traditionally periodic square honeycomb metamaterials, the aperiodically arranged hat honeycomb metamaterials exhibit superior mechanical properties.

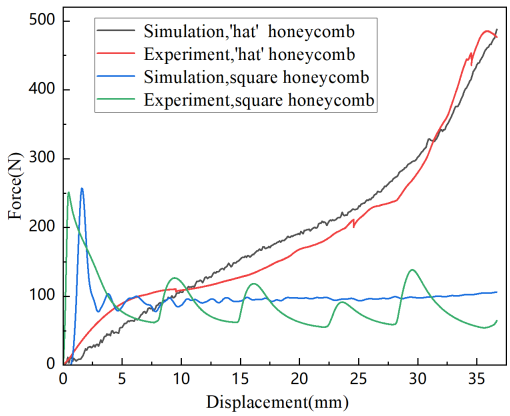

Figure 14. Comparison of force-displacement curves between finite element simulations and experiments.

4.2. Absorption Performance Analysis

Specific energy absorption (SEA) is a common index to assess the energy absorption of a structure. The value of SEA is proportional to the energy absorption capacity of the structure.SEA generally indicates the energy absorbed per cell element mass and can be written as:

$$SEA = \frac{EA(\varepsilon)}{M} \tag{8}$$

where $EA(\varepsilon)$ is the energy absorbed when the axial deformation is ε. M is the weight of the energy-absorbing structure. Based on Eq.8, the relationship between the energy absorption per unit mass and the nominal strain of the hat honeycomb and square honeycomb metamaterials, including both experimental and simulated results, is shown in Figure 15. Under quasi-static compression, the hat honeycomb structure may perform better in terms of energy absorption because it can maintain a higher load-bearing capacity at larger displacements. In contrast, the force in the square honeycomb structure may increase more rapidly at large displacements, followed by a rapid structural instability and a decrease in load-bearing capacity, resulting in relatively lower energy absorption capability. In summary, compared to the traditionally periodic square honeycomb metamaterials, the aperiodically arranged hat honeycomb metamaterials exhibit superior energy absorption performance, making them suitable for applications that require high strength and toughness.

 doi:10.20944/preprints202407.1532.v2

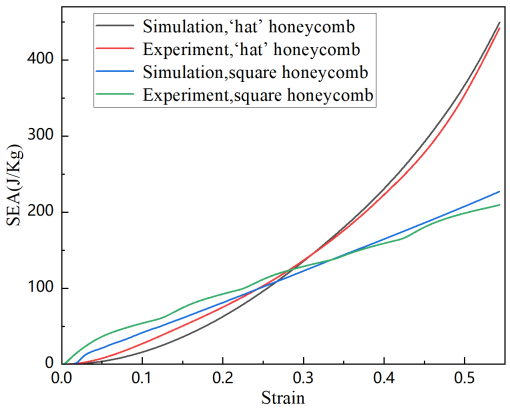

Figure 15. Energy absorption versus nominal strain relationship of two honeycomb metamaterials at room temperature.

5. Conclusions and Perspectives

The question is why the mechanical properties of disordered structures are superior to those of ordered structures. The essential reason is that the most disordered state is actually the most natural state. The so-called statistical equilibrium state is the state where entropy reaches its maximum value (i.e., a high-entropy state). The equilibrium state is the most disordered state, which is also the most natural state. Therefore, high-entropy structures possess superior mechanical characteristics.

Through the study of structural mechanics derived from the Einstein cell puzzle, therefore, the following conclusion can be drawn. The non-periodic structures generated by introducing disorder exhibit superior mechanical properties compared to periodic structures, and the underlying reason for this is that non-periodic structures generally have high information entropy. By utilizing the information entropy of structures, it is possible to qualitatively predict the mechanical properties of materials without the need for experimental or computational simulations. Therefore, this research aids in the structural design of materials. It is particularly noted that, to the best of the author's knowledge, this paper is the first to propose a definition of topological entropy from an information-theoretic perspective. Such theoretical research should be considered a theoretical contribution to the design of metamaterials.

Conflicts of Interest: The authors declare that there are no competing financial interests.
Availability of data: There is no data in this study.

References

1. E. Conover, Mathematicians have finally discovered an elusive 'einstein' tile, Science News, April 24, 2023.
2. Smith, D., Myers, J. S., Kaplan, C. S. Goodman-Strauss, C. An aperiodic monotile, arXiv preprint arXiv:2303.10798 (2023).
3. C. S. Kaplan, Private commumication, 21 June, 2023.
4. D. Shechtman, et al. Metallic phase with long-range orientational order and no translational symmetry. Phys. Rev. Lett. 53, 1951 (1984).
5. I. Georgescu, 50 years of Penrose tilings, Nat Rev Phys 6, 408 (2024).
6. K. Bertoldi, V. Vitelli, J. Christensen & M. van Hecke, Flexible mechanical metamaterials. Nat. Rev. Mater. 2, 17066 (2017).
7. M. Ashby, The properties of foams and lattices. Phil. Trans. R. Soc. A 364, 15-30 (2006).
8. R. Lakes, Foam structures with a negative Poisson's ratio. Science 235, 1038, C1040 (1987).
9. M. Hanifpour, C.F. Petersen, M.J. Alava & S. Zapperi, Mechanics of disordered auxetic metamaterials. Eur. Phys. J. B 91, 271 (2018).
10. M. Zaiser and S. Zapperi, Disordered mechanical metamaterials, Nat Rev Phys 5, 679-688 (2023).
11. D. Tüzes, P.D. Ispanovity & M. Zaiser, Disorder is good for you: the influence of local disorder on strain localization and ductility of strain softening materials, Materials Today, Volume 73, March/April 2024.

 doi:10.20944/preprints202407.1532.v2

12. S. Bonfanti, R. Guerra, F. Font-Clos, D. Rayneau-Kirkhope & S. Zapperi, Automatic design of mechanical metamaterial actuators. Nat. Commun. 11, 4162 (2020).
13. K. Liu, R. Sun, & C. Daraio, Growth rules for irregular architected materials with programmable properties. Science 377, 975-981 (2022).
14. Q.W. Li, B.H. Sun, Optimization of a lattice structure inspired by glass sponge. Bioinspiration & Biomimetics, 18(1): 016005 (2022).
15. Q.W. Li, B.H. Sun, Numerical analysis of low-speed impact response of sandwich panels with bio-inspired diagonal-enhanced square honeycomb core. International Journal of Impact Engineering, 173, 104430 (2023).
16. F. Wu and B.H. Sun, Study on functional mechanical performance of array structures inspired by cuttlebone. Journal of the Mechanical Behavior of Biomedical Materials, 136, 105459 (2022).
17. X.L. Guo and B.H. Sun, Detachable connection mechanics of thin-walled cylindrical snap fit docking. Extreme Mechanics Letters, 67, 102122 (2024).
18. X.L. Guo and B.H. Sun, Mechanics of a thin-walled segmented torus snap fit. Thin-Walled Structures, 198, 111676 (2024).
19. J. Wei and B.H. Sun, Bioinspiration: Pull-Out Mechanical Properties of the Jigsaw Connection of Diabolical Ironclad Beetle's Elytra, Acta Mech. Solida Sin. 36, 86, C94 (2023).
20. J. Wei and B.H. Sun, Study on the mechanical properties of cylindrical mechanical metamaterials with biomimetic honeycomb units of the diabolical ironclad beetle, Extreme Mechanics Letters, 67 102127 (2024).
21. D.J. Clarke, F. Carter, I. Jowers, R.J. Moat, An isotropic zero Poisson's ratio metamaterial based on the aperiodic hat monotile, Applied Materials Today, 35 101959 (2023).
22. R.J. Moat et al., A class of aperiodic honeycombs with tuneable mechanical properties, Aplied Materials Today, 37 102127 (2024).
23. X.X. Wang, et al. Unprecedented Strength Enhancement Observed in Interpenetrating Phase Composites of Aperiodic Lattice Metamaterials, Adv. Funct. Mater, 2406890 2024.
24. M.M. Naji and R.K. Abu Al-Rub, study the effective elastic properties of novel aperiodic monotile-based lattice metamaterials, Materials & Design, 244 113102(2024).
25. J. Jung, A.L. Chen, G.X. Gu, Aperiodicity is all you need: Aperiodic monotiles for high-performance composites. Materials Today. 73, 1-8 (2024).
26. B.H. Sun, High-entropy structural mechanics, Lect. 25, a series seminar of Inst. of Mechanics and Technology, Xi'an Uni. of Architecture and Technology, 26 Oct. 2023. https://imt.xauat.edu.cn/info/1008/3763.htm
27. B.H. Sun, Thermodynamics and high-entropy structural mechanics, Lect. 27, a series seminar of Inst. of Mechanics and Technology, Xi'an Uni. of Architecture and Technology, 15 Nov. 2023. https://imt.xauat.edu.cn/info/1008/3801.htm
28. C.E. Shannon, A mathematical theory of communication, Bell Syst. Tech. J., vol. 27, 379-423, 623-656, July-Oct. 1948.